Vortex evolution on a nonslender delta wing

Aadil Manazir[1], Kevin Wabick[2], Brian Snider[2], Austin Krebill[2], James Buchholz[2], PhD
[1]Pleasant Valley High School, Bettendorf, IA, [2]College of Engineering, University of Iowa

Background

In the future, unmanned supersonic aircraft will soar the skies. These aircraft generally incorporate the triangular delta wing. The delta wing can be divided into two categories, slender and nonslender, with nonslender wings having sweep angles under 55°. An aspect of nonslender flight recently attracting more attention is the leading edge vortex. The leading edge vortex is complicated: it can have secondary and tertiary vortices, and it has the potential to generate lift. Additionally, the vortex evolves throughout the wing, getting stronger or weaker. In the present project, the factors governing vortex evolution, diffusive flux, out of plane flux, and shear layer flux are explored at different Reynold's numbers.

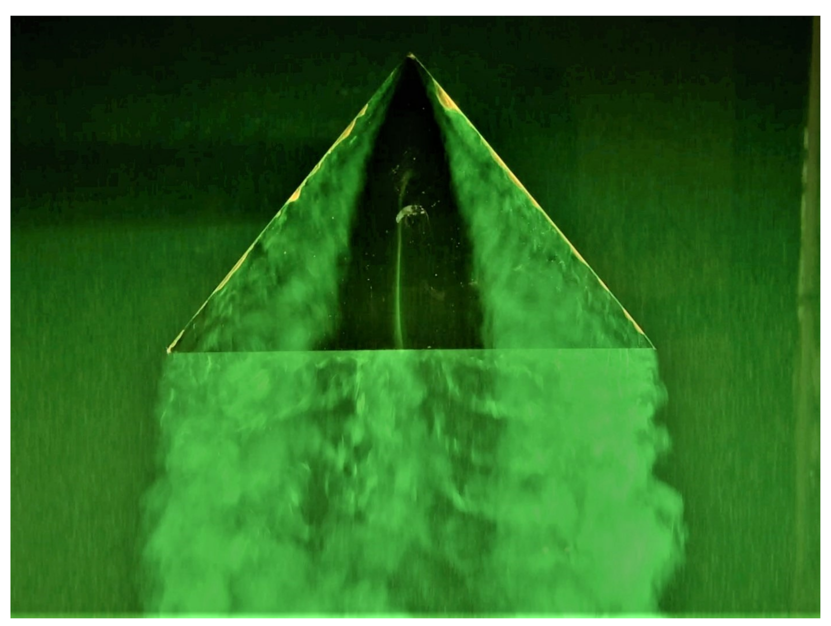

Figure 1: Leading edge vortex visualized with fluorescein dye mixed with Elmer's glue.

Objective

Use the vorticity transport equation to quantify the sources and sinks of vorticity contributing to leading edge vortex instability on a nonslender delta wing at an angle of attack of 12° for various Reynold's numbers.

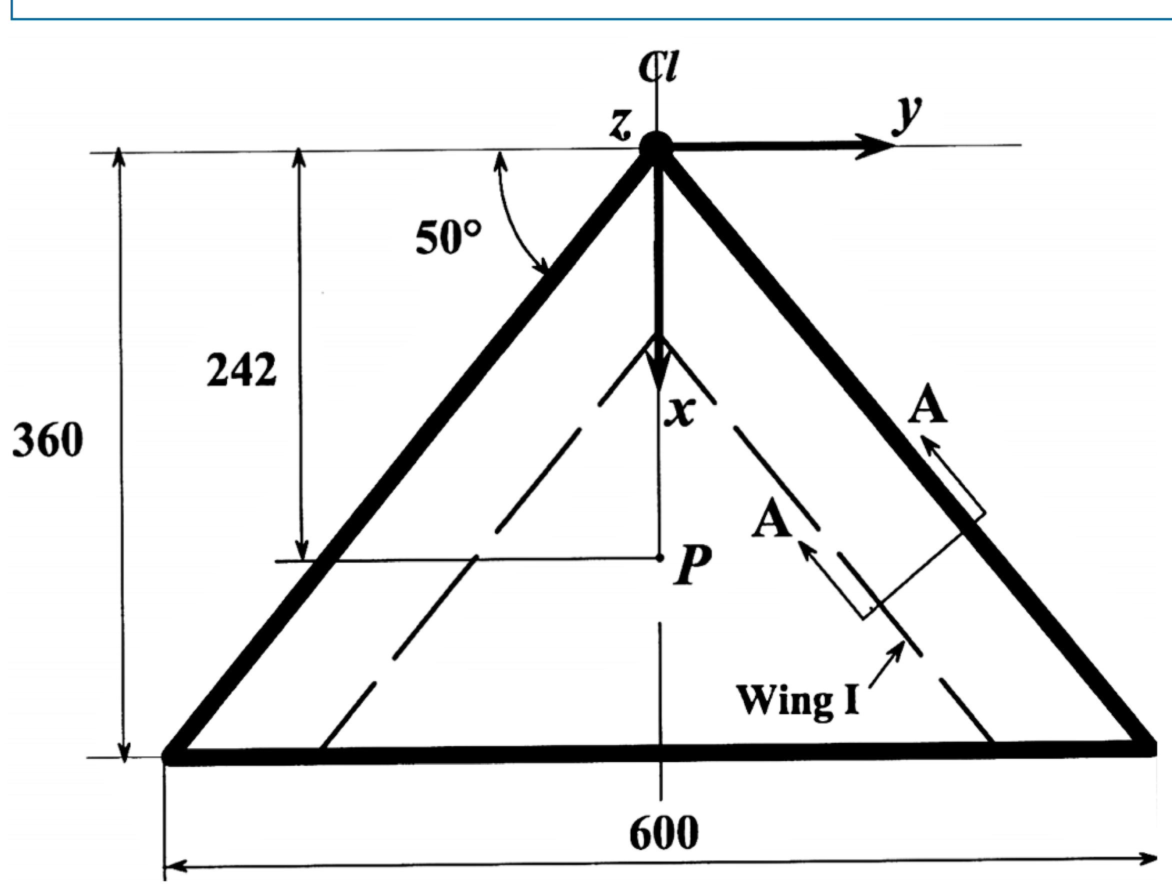

Figure 2: Drawing of the delta wing used, taken from Verhaagen's experiment [1]. Measurement units are 1/100 in.

Method

The wing's design was taken from a previous experiment done by Verhaagen[1] (see figure 2). The wing was then 3-D modeled in Autodesk Inventor and created out of aluminum. Next, the wing was placed in a flume with a low pump speed at an angle of attack of 12°. Particle tracking velocimetry was used for data collection, with LaVision mini shaker cameras imaging small nylon particles in the flow and DaVis 10 software interpreting the images. 2 more data sets were collected at different pump speeds. Finally, the vorticity transport equation (see figure 3) was applied to the data sets using in-house code for flux analysis.

Figure 3: Vorticity transport equation used for flux analysis

$$\frac{d\Gamma}{dt} \approx \overbrace{\left\{\int_A \left(\omega_x \frac{\partial u_z}{\partial x} + \omega_y \frac{\partial u_z}{\partial y} - u_z \frac{\partial \omega_z}{\partial z}\right) dA\right\}}^{\text{Out of plane flux}} \overbrace{\left\{+\frac{1}{\rho}\int_4 \frac{\partial P}{\partial x} dx\right\}}^{\text{Diffusive flux}}$$

$$\overbrace{\left\{-\oint_{\partial A} (\vec{u}\cdot\hat{n}_{\partial A})\,\omega_z ds\right\}}^{\text{Shear layer flux}}$$

Results

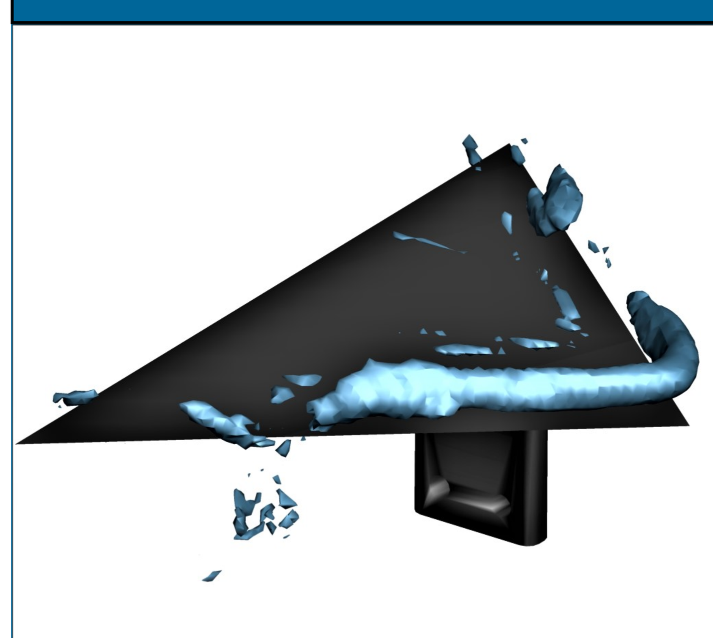

Figure 4: Isosurface showing vorticity at Reynold's number 20000

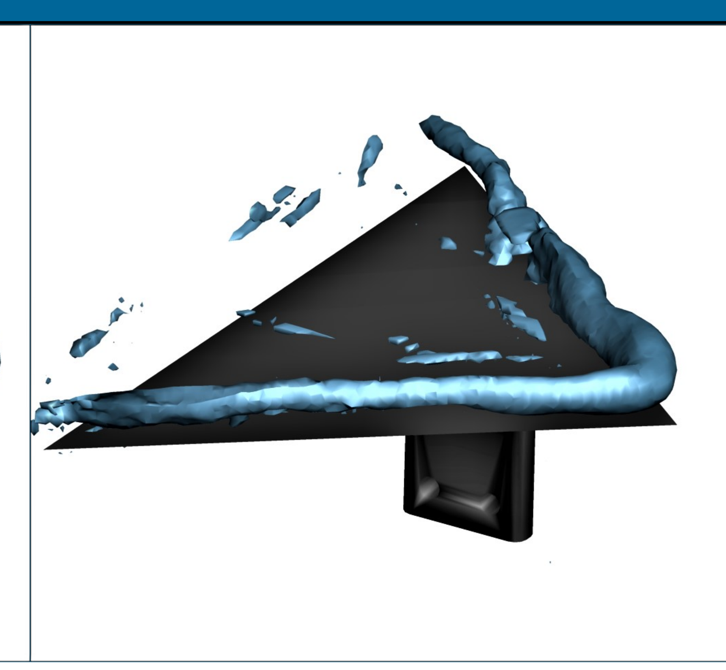

Figure 5: Isosurface showing vorticity at Reynold's number 29000

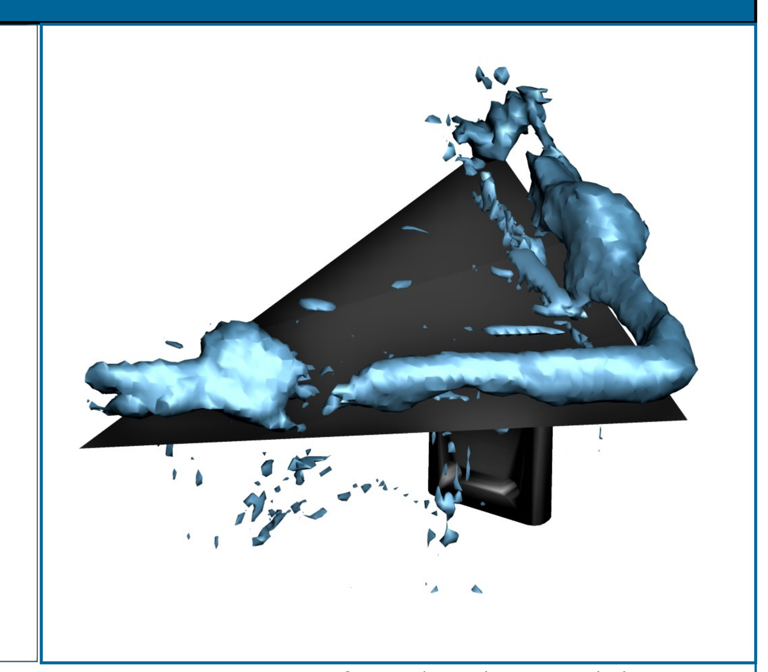

Figure 6: Isosurface showing vorticity at Reynold's number 38000

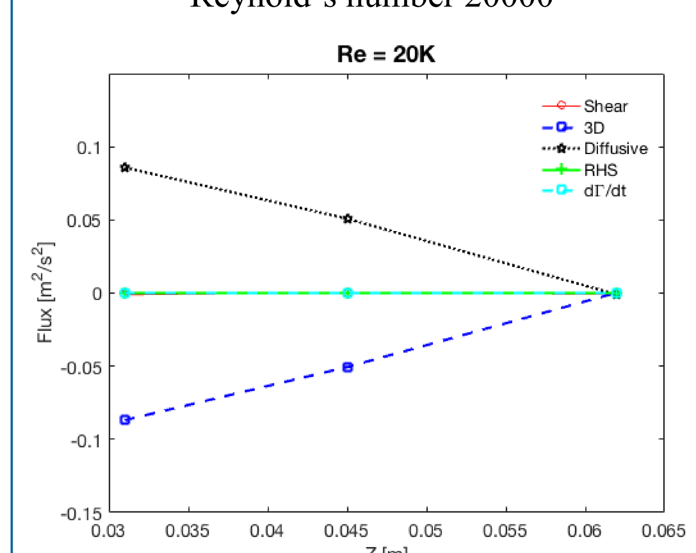

Figure 7: Flux levels at different z coordinates on the wing at Reynold's number 20000

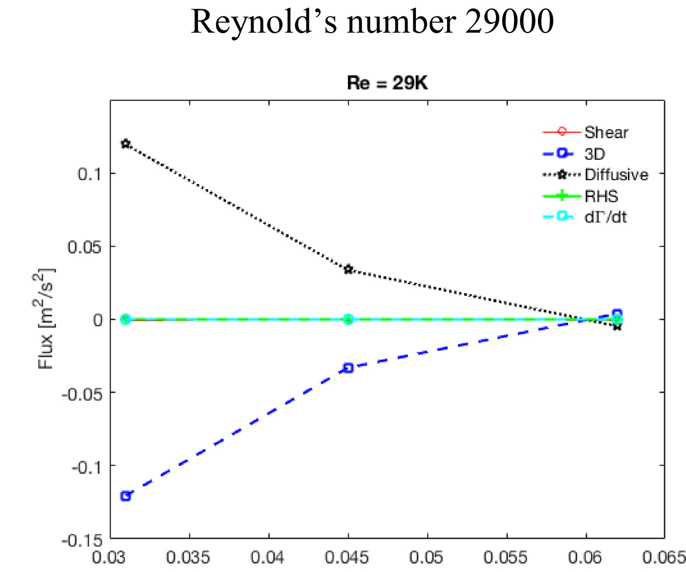

Figure 8: Flux levels at different z coordinates on the wing at Reynold's number 29000

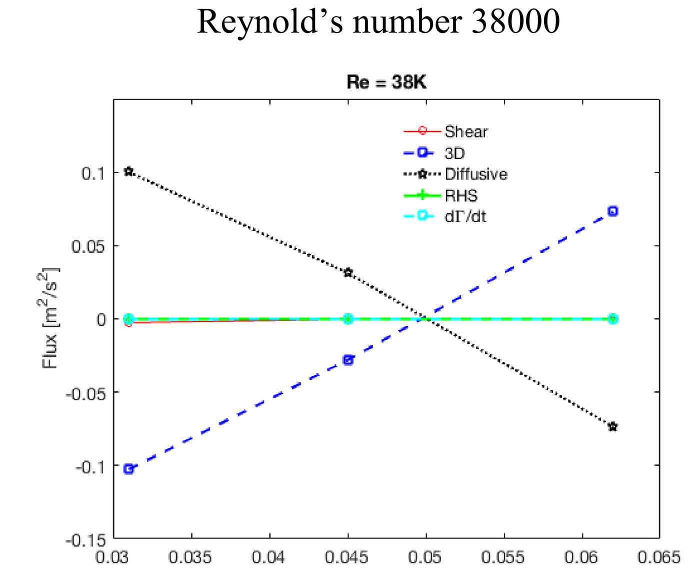

Figure 9: Flux levels at different z coordinates on the wing at Reynold's number 38000

Vorticity's sensitivity to Reynold's number is seen through the variance in isosurfaces. Vortex breakdown is observed at Reynold's number 38000. Slight asymmetry in isosurfaces may be due to a miniscule tilt in the wing during testing.

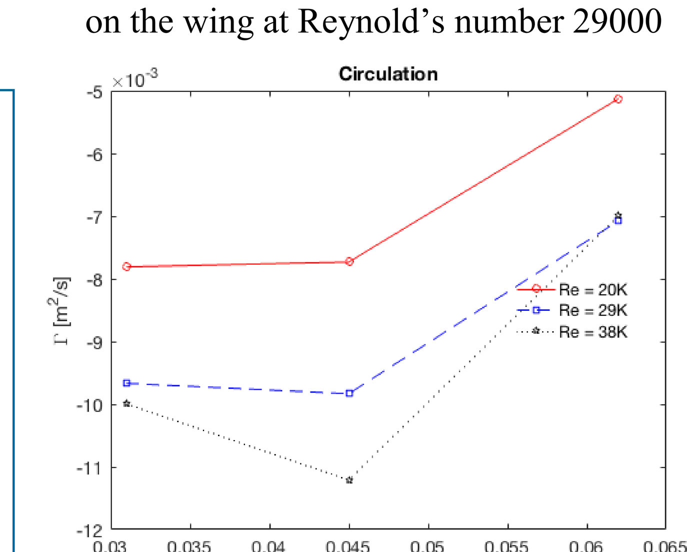

Figure 10: Circulation at different z coordinates for Reynold's numbers 20000, 29000, and 38000

Flux sensitivity to Reynold's number is seen through the variance in flux values. Due to direction of circulation, negative flux values are sources of vorticity and positive flux values are sinks of vorticity.

Conclusions

Contrary to expectations, for our data range, the magnitude of circulation generally decreases as one moves downstream. It then follows that the vortex strengthens from the apex over a small streamwise distance, then starts to weaken. For Reynold's number 38000, however, the magnitude of circulation increases for a much longer distance. For Reynold's numbers 20000 and 29000, 3-D (out of plane) flux is a source of vorticity, corresponding to decreasing in circulation magnitude. Conversely, at Reynold's number 38000, where circulation magnitude is increasing, 3-D flux is still a source. Additionally, at that Reynold's number, 3-D flux goes from a source to a sink and diffusive flux vice versa. Except when diffusive and 3-D flux cross, diffusive flux is a sink. Different than other airflow cases, shear layer flux isn't the main contributor to vorticity. Circulation magnitude increases as Reynold's number increases.

Future Implications

Future experiments should confirm that the shear layer flux is significantly less in magnitude than the 3-D and diffusive flux. Further analysis and possibly data collection is necessary to understand the correspondence of 3-D flux being a source of vorticity and circulation increasing in magnitude, and the possible relation between vortex breakdown and 3-D and diffusive flux changing signs.

Acknowledgements

I'd like to thank Dr. James Buchholz for giving me the opportunity to research in the fluids lab. I'd also like to thank Brian Snider, Kevin Wabbick, and Austin Krebill for guiding me through the research process. A special thanks to the Belin-Blank center for supporting the SSTP program.

References

Gursul, I. (2005). Unsteady Aerodynamics of Nonslender Delta Wings. Progress in Aerospace Sciences, *Science Direct, 41*, 515–557

Panah, A., Akkala, J., Buchholz, J. (2015). Vorticity transport and the leading-edge vortex of a plunging airfoil. *Experiments in Fluids, 56,* 160-175.

Verhaagen, N. (2012). Leading-Edge Radius Effects on Aerodynamic Characteristics of 50-Degree Delta Wings. *Journal of Aircraft 49*, 521-531.